Zinc isotope fractionation during the sorption of Zn to minerals and organic matter in sediment cores affected by anthropogenic pollution

Kai Nils Nitzsche [a],[*],[1], Toshihiro Yoshimura [a], Naoto F. Ishikawa [a], Hodaka Kawahata [b],[c], Nanako O. Ogawa [a], Katsuhiko Suzuki [d], Daisuke Araoka [b], Naohiko Ohkouchi [a]

[a] Biogeochemistry Research Center, Japan Agency for Marine-Earth Science and Technology (JAMSTEC), 2-15 Natsushima-cho, Yokosuka, Kanagawa, 237-0061, Japan
[b] Geological Survey of Japan, National Institute of Advanced Industrial Science and Technology, 1-1-1 Higashi, Tsukuba, Ibaraki, 305-8567, Japan
[c] Atmosphere and Ocean Research Institute, The University of Tokyo, 5-1-5 Kashiwanoha, Kashiwa, Chiba, 277-8564, Japan
[d] Submarine Resources Research Center, Japan Agency for Marine-Earth Science and Technology (JAMSTEC), 2-15 Natsushima-cho, Yokosuka, Kanagawa, 237-0061, Japan

ARTICLE INFO

ABSTRACT

Zinc stable isotopes (δ^{66}Zn) serve as a widely fingerprinting tool for detecting anthropogenic Zn contamination. However, there is a limited understanding of δ^{66}Zn behavior during the sorption of Zn to minerals and organic matter. In this study, we have determined the δ^{66}Zn values in specific fractions to investigate their effectiveness in tracing anthropogenic Zn. The revised Community Bureau of Reference (BCR) extraction procedure was applied to a coastal marine core from Osaka Bay and from a lacustrine core from Lake Biwa, both with a history of anthropogenic metal pollution. The δ^{66}Zn values varied from −0.14 ‰ to +1.00 ‰ across the four to five chemical fractions with up to 0.9 ‰ variation within a single horizon. The highest δ^{66}Zn values in the acid-soluble fraction (up to +1.00 ‰) could be explained by the preferential sorption of ^{66}Zn to carbonates and/or the preferential incorporation of ^{66}Zn into calcite. The complex isotopic fractionation during the sorption of Zn to and co-precipitation with Fe–Mn oxyhydroxides likely resulted in an unclear pattern of the δ^{66}Zn values of the reducible fraction. Low δ^{66}Zn values in the oxidizable fraction (Osaka Bay) agree with the ^{64}Zn enrichment in phytoplankton. Higher δ^{66}Zn values of the reducible and oxidizable fractions of the Lake Biwa core indicate that environmental conditions (e.g. ionic strength) and for instance different phytoplankton species or dissolved and suspended particulate matter input drive the Zn isotope fractionation depending on the system (marine vs. lacustrine). The δ^{66}Zn values of the acid-soluble fraction (Osaka Bay and Lake Biwa), of the reducible fraction (only Lake Biwa) and of oxidizable fraction (only Osaka Bay) better reflected the temporal changes in the Zn concentration than the bulk sediment, indicating that these fractions could be a sensitive fingerprinting tool for anthropogenic Zn contamination.

1. Introduction

Marine and lacustrine sediments from the suburbs of human settlements can be used to reconstruct time series changes covering historical periods (Araújo et al., 2017, 2019; Gao et al., 2018; Hornberger et al., 1999; Nitzsche et al., 2021, 2022; Sakata et al., 2019; Thapalia et al., 2010, 2015; Wang, Gao et al., 2022). Trace metals in such sediments are present in different mineral and organic phases or sorbed to their surfaces including exchangeable metals in interlayers of clays, as part of or

sorbed to carbonates and organic matter, complexed with humic acids, sorbed to surfaces of Fe–Mn oxyhydroxides and of sulfides, and as part of the crystal lattice of silicates. Over the past two decades, "trace metal" isotope systems such as copper (Cu), zinc (Zn) and mercury (Hg) have become a popular fingerprinting tool to trace anthropogenic metals in aquatic (Araújo et al., 2022) and terrestrial (Bigalke et al., 2010; Sullivan et al., 2022; Wang, Zheng et al., 2022) environments. In particular, anthropogenic Zn sources have been assessed based on Zn stable isotope analysis of surface sediments and sediment cores from lacustrine

(Nitzsche et al., 2021; Thapalia et al., 2010, 2015; Tonhá et al., 2021; Xia et al., 2023) and marine environments (Araújo et al., 2017, 2019; Jeong et al., 2023; Nitzsche et al., 2022; Sakata et al., 2019; Tonhá et al., 2020). These studies often assume a binary mixing between an anthropogenic endmember enriched or depleted in ^{66}Zn depending on the source with a natural endmember (Araújo et al., 2017, 2019; Nitzsche et al., 2021, 2022; Sakata et al., 2019; Tonhá et al., 2020).

Yet, most of these studies have determined the δ^{66}Zn values in bulk sediments ignoring the potential effects of post-emission processes such as isotopic fractionation during the sorption of Zn to mineral surfaces and organic matter in the terrestrial environment, in the water column and in the diagenetically altered sediment (Komárek et al., 2022), which could hamper the use of δ^{66}Zn values as anthropogenic tracers (Zimmermann et al., 2020). Overall, the Zn isotopic fractionation during sorption (Δ^{66}Zn = δ^{66}Zn$_{solid}$−δ^{66}Zn$_{solution}$) to mineral and organic surfaces ranges from −0.28 to +1.04 ‰, thus mostly favoring the heavy ^{66}Zn isotope due to the difference in stability between its free aqueous and sorbed Zn forms (Balistrieri et al., 2008; Bryan et al., 2015; Dong and Wasylenki, 2016; Gélabert et al., 2006; Juillot et al., 2008; Komárek et al., 2022; Nelson et al., 2017; Pokrovsky et al., 2005; Wang et al., 2023; Yan et al., 2023). Such fractionation factors are typically derived from sorption experiments using different ionic strengths, pH values, and Zn concentrations until equilibrium conditions are reached. Yet, the dominant sorption processes in sediments are largely unknown which can be considered as open systems with a number of cations (e.g. Na$^+$, Ca^{2+}) and anions (e.g. Cl$^-$, SO$_4^{2-}$) present in the overlying water column and pore water, varying redox conditions and different primary producers.

Operational trace metal speciation is achieved by using different extraction reagents sequentially applied to a sample (sequential extraction - SE) (Bacon and Davidson, 2008; Hass and Fine, 2010). Such methods can provide insights into the potential mobility and bioavailability of trace metals and the preferential binding of anthropogenic Zn by combining Zn concentrations with δ^{66}Zn values in specific fractions. Thapalia et al. (2010) attributed low δ^{66}Zn values (−0.03 ± 0.08 ‰) in an acid-labile fraction (supposed to target Fe oxides) in a sediment core from an urban lake to urban runoff depleted in ^{66}Zn. Tonhá et al. (2020) found higher δ^{66}Zn values (+1.03 ± 0.12 ‰) in the acid-soluble fraction (targeting at exchangeable species and carbonates) compared to the bulk surface sediments (+0.67 ± 0.18 ‰) in a coastal bay. Tonhá et al. (2020) suggested that Zn from electroplating waste being typically enriched in ^{66}Zn (Kavner et al., 2008) explained such an ^{66}Zn enrichment in the acid-soluble fraction, but could not rule out the ^{66}Zn enrichment due to the precipitation of carbonates. The latter can be enriched in ^{66}Zn depending on the carbonate type (Dong and Wasylenki, 2016; Mavromatis et al., 2019; Müsing et al., 2022). Thus, although a preferential sorption of anthropogenic Zn to specific minerals is possible, isotopic fractionation during the sorption must be considered as well.

We have sequentially extracted Zn from two sediment cores from lacustrine Lake Biwa and from coastal Osaka Bay and determined their bulk δ^{66}Zn values (Nitzsche et al., 2021, 2022). The increase in the Zn concentration in Osaka Bay sediment core from the 1870s AD and peak during the early 1960s AD resulted from various industrial and urban activities in the catchment including coal combustion, ore smelting and industrial and domestic wastewaters (Nitzsche et al., 2022; Yasuhara and Yamazaki, 2005). Regarding Lake Biwa, industrial and domestic wastewaters and other diffusive sources (e.g. road runoff) contributed to increasing Zn concentrations from the late 1950s (Nitzsche et al., 2021). Yet, changes in the Zn concentrations do not allow for drawing conclusions on the Zn sources. Slight decreases of ~0.1 ‰ in the δ^{66}Zn values from the 1950s towards the surface indicated the contribution of an urban, industrial Zn source depleted in ^{66}Zn (Nitzsche et al., 2021, 2022). However, the δ^{66}Zn values were not in a good agreement with the corresponding Zn concentrations. We found that the anthropogenic Zn was mostly hosted in the acid-soluble and reducible fractions. Thus, the

main goal of the present study was to test, if the δ^{66}Zn values of the acid-soluble and of the reducible fractions better reflected the change in Zn concentrations than the bulk sediment. Furthermore, we aimed for explaining the variation in the δ^{66}Zn values across the different metal fractions by means of Zn isotopic fractionation during incorporation in and sorption to minerals and organic matter. The coupling of Zn stable isotopes directly measured on operationally defined fractions provide new insights into the preferential binding of anthropogenic Zn while considering Zn isotope fractionation during the sorption of Zn.

2. Material and methods

2.1. Study site

The catchment of Osaka Bay is located in central Japan and covers a total area of approximately 10,700 km^2 with the Yodo River catchment being the largest (8240 km^2). The catchment is Osaka Bay is covered by forest; yet large urban and build-up land areas are present owing to the Kyoto-Osaka-Kobe (Keihanshin) metropolitan area. The bedrock of the whole catchment consists mainly of Quaternary unconsolidated sediments (Itihara et al., 1988), clastic (meta)sedimentary rocks of the Jurassic and Cretaceous accretionary complexes, Cretaceous granitoid rocks, felsic volcanic and volcanoclastic rocks, and minor gneisses and schists, Carboniferous to Permian limestones and basalts, and Cretaceous gabbro (Nitzsche et al., 2022).

Lake Biwa is located in the NE area of the catchment and consists of an up to 104 m deep (average depth 44 m), 616 km^2 large, mesotrophic northern basin, and an up to 8 m deep (average depth 3.5 m), 58 km^2 small, eutrophic southern basin (Fig. 1). 118 tributaries discharge into the lake and the Seta River (upper part of the Yodo River) in the southern basin is the only outflow. Farmland is mostly present in the SE of Lake Biwa.

Rapid industrialization, urbanization and population growth took place in Osaka City from about 1890 (the start of Japan's industrial revolution) and during Japan's post-war period of economic growth (1955–1973). The latter led to rapid urbanization and industrialization in the southern catchment of Lake Biwa. Industrial effluents were strictly regulated from the late 1960s, and mineral fertilizers, irrigation water for agriculture, livestock wastes and domestic wastewaters from the late 1970s. From the 1980s, wastewater treatment plants and a sewerage system were constructed (Petts, 1988).

2.2. Sediment sampling

The sampling and preparation of the sediment core from Lake Biwa have been reported before (Ogawa et al., 2001). Briefly, a 46 cm long sediment core was collected with a gravity corer from the northern basin at a water depth of 85 m in 1995 (Fig. 1). The core was cut in 0.5-cm slices from the surface to a depth of 12 cm. The sediment samples were oven-dried at 60 °C and ground.

Nitzsche et al. (2022) reported the sampling and preparation of the sediment core from Osaka Bay. Briefly, a piston core was collected at station OS5B from the central part of Osaka Bay at a water depth of 24 m during the cruise KT-11-13 on July 1, 2011. The core was cut in 2-cm slices from the surface to the final core depth of 884 cm. Sediment samples were freeze-dried, sieved to <125 μm, and manually powdered.

2.3. Core dating

The sediment core from Lake Biwa has been dated using ^{210}Pb (Ogawa et al., 2001), and the age of the 13.7 cm depth extrapolated to 1850 (Nitzsche et al., 2021).

The Osaka Bay core has been dated by radiocarbon measurement of molluscan shells using accelerator mass spectrometry (AMS) at the Micro Analysis Laboratory of the University of Tokyo (Matsuzaki et al., 2004; Yokoyama et al., 2019). The employed technique for sample
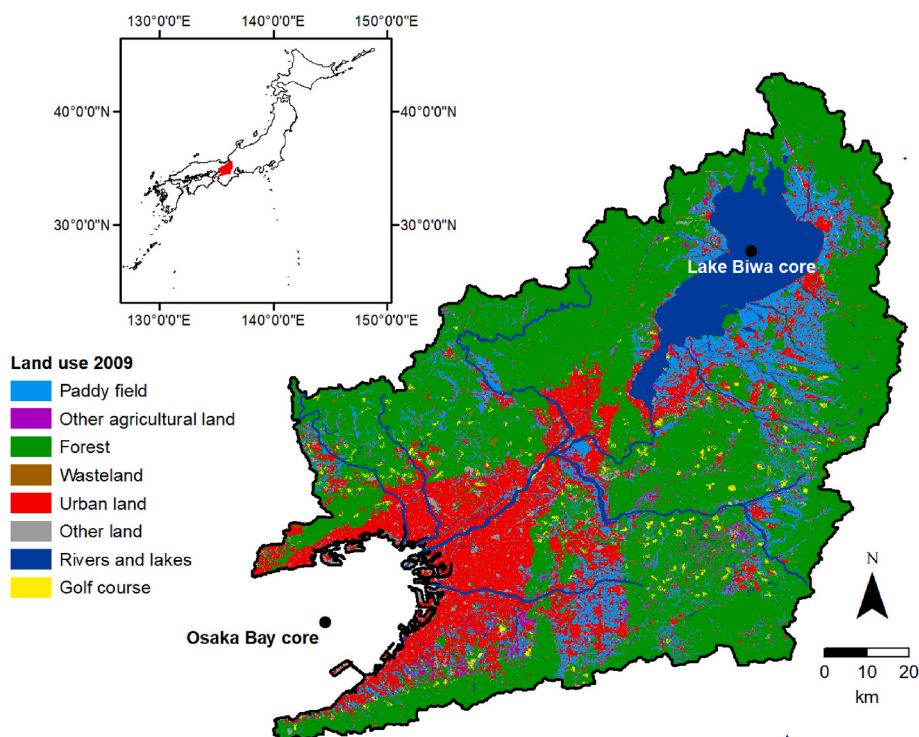
Fig. 1. Location of the Osaka Bay catchment in Japan, and land-use map with the locations of the sediment core collected in Osaka Bay (KT-11-13 OS5B) and in Lake Biwa. Land-use data were obtained from Land Use Fragmented Mesh Version 2.5.1 from the National Land Numerical Information, created by the Ministry of Land, Infrastructure, Transport and Tourism, the Government of Japan.

preparation has been previously reported (Nitzsche et al., 2022; Yokoyama et al., 2007). The radiocarbon age results were calibrated to calendar years using the OxCal ver. 4.4 software (Bronk Ramsey, 2009) with the Marine 20 dataset (Heaton et al., 2020) assuming a regional specific reservoir (DR) correction of 135 ± 20 years (Kuwae et al., 2013). The core provided a continuous environmental record of the last 2300 years; yet, for the current study, we focus on the last 300 years.

2.4. X-ray diffraction analysis

We conducted powder XRD analyses of selected samples from the Lake Biwa core (n = 6) and from the Osaka Bay core (n = 6) to identify the main minerals in the samples. The powdered samples were analyzed using a Rigaku Smart Lab X-ray diffractometer (40 kV operating voltage and 200 mA current) at the Geological Survey of Japan (GSJ), National Institute of Advanced Industrial Science and Technology (AIST) according to Araoka et al. (2022). The samples were scanned from $3°$ to $70°$ 2θ with a step size of $0.02°$ and a scan speed of $1° \, \mathrm{min}^{-1}$. Minerals identification using the obtained data was conducted by PDXL database fitting program (ver. 2.9.1.0). Before sample measurements, a quartz standard sample was analyzed for the reference of diffraction peak positions. The semi-quantitative results were obtained by comparing area intensities of the strongest diffraction peaks of each mineral (Miyoshi et al., 2015).

2.5. Total organic carbon analysis

The total organic carbon (TOC) content of the Osaka Bay core samples was determined after weighing samples into pre-cleaned smoothed wall tin capsules, decalcification with 0.5M HCl and drying on a hotplate at 80 °C. The tin capsules were sealed, and analyzed by a sensitivity improved elemental analyzer (Flash EA1112, Thermo Finnigan, Bremen, Germany) connected to an isotope ratio spectrometer (Delta plus XP, Thermo Finnigan, Bremen, Germany) at the Biogeochemistry Research Center (BGC), JAMSTEC, according to Ogawa et al. (2010). Some TOC

concentrations of selected horizons have been shown in our previous study (Nitzsche et al., 2022). The TOC contents of the Lake Biwa core samples have been reported before (Ogawa et al., 2001).

2.6. Sequential extraction

The Commission of European Communities' Community Bureau of Reference (BCR) sequential extraction (SE) scheme, referred to as the revised BCR method (Rauret et al., 1999; Sahuquillo et al., 1999), is well-known and widely applied, in which trace metals are extracted with the extraction reagents chosen to mimic changes in environmental conditions (e.g. inducing acidification or reducing conditions). The SE procedure has been reported in our previous studies (Nitzsche et al., 2021, 2022). Briefly, Zn has been extracted from selected sediment horizons (Osaka Bay: n = 56; Lake Biwa: n = 19) using a slight modification of the revised BCR method (Table 1). Single extractions were performed using 100 mg sample while maintaining the same sample-/solution ratios, the supernatant was removed by pipetting, and the residue was washed three times with methanol and evaporated to dryness at 60 °C. For the Lake Biwa core, water-soluble and exchangeable metals were extracted with 1M NH_4Cl as the first step. Instead for the Osaka Bay core, only ten samples were extracted with 1M NH_4Cl to test for exchangeable metals. For the Osaka Bay core, the extraction with 0.11M acetic acid was repeated to ensure a complete extraction of the acid-soluble fraction as we have observed the pH still declined during a second acetic acid extraction indicating that carbonates were still present after only one extraction. Reproducibility was assessed by replicate extraction analysis of the JLk-1 sediment reference material (n = 3) and of the Tokyo Bay sediment JMS-1 reference material (n = 4). The Zn recovery ranged from 95 % to 100 % with respect of the certified values.

2.7. Chemical and isotopic analyses

Aliquots of the extracts were analyzed for elemental concentrations using a quadrupole inductively coupled plasma mass spectrometry

Table 1
Overview of the sequential extraction procedure with nominal target phases.

Core	Fraction	Target phases	Extractant
Lake Biwa	Exchangeable	Soluble and exchangeable species	1M NH_4Cl
Lake Biwa, Osaka Bay	Acid soluble #1	Carbonates	0.11M CH_3COOH
Osaka Bay	Acid soluble #2	Carbonates	0.11M CH_3COOH
Lake Biwa, Osaka Bay	Reducible	Fe–Mn oxyhydroxides	0.5M $NH_2OH \cdot HCl$, pH = 1.5
Lake Biwa, Osaka Bay	Oxidizable	Organic matter and sulphides	8.8M H_2O_2 (two times) followed by 1M CH_3COONH_4, pH = 2
Lake Biwa, Osaka Bay	Residual	Silicates, well-crystalline oxides	HNO_3–HF–$HClO_4$

(iCAP Q ICP-MS; Thermo Scientific, Bremen, Germany) at JAMSTEC. The results have been reported in our previous works (Nitzsche et al., 2021, 2022).

The Zn concentrations in the exchangeable fraction were typically <1 % of the bulk sediment for Lake Biwa and <3 % of the bulk sediment for Osaka Bay (Nitzsche et al., 2021, 2022); thus, the exchangeable fraction was considered negligible for the current study.

High purity HCl and HNO_3 (Ultrapur-100, Kanto Chemical) and double-deionized water (DW), purified using a Milli-Q Gradient-A10 system (Merck Millipore), were used for the purification of Zn. The extracts from selected horizons (Osaka Bay: n = 10; Lake Biwa: n = 8) were evaporated, digested in mixtures of HNO_3 and H_2O_2 to remove organics (except for the residual fraction), evaporated again and dissolved in 1 mL of 6M HCl prior to loading on the columns. Zinc was purified from solutions with BioRad AG1-X8 anion-exchange resin (200–400 mesh) in chloride form using a modified version of the protocol described in Sossi et al. (2015). Briefly, Zn was eluted with 2 mL of double-deionized water after washing the resin with 5 mL of 8M HCl, 5 mL of 3M HCl and 4 mL of 0.4M HCl. The final Zn extract was evaporated to dryness, re-dissolved in 0.5 mL HNO_3 and 0.05 mL H_2O_2 and heated at 140 °C to digest organics from the resin, again evaporated to dryness, and finally redissolved in 2 % HNO_3.

The purified samples were diluted to 2 % HNO_3 and a concentration of 200 ppb. Zinc stable isotope ratios were measured on these solutions under wet plasma conditions with low-resolution mode using a Neptune Plus Multicollector ICP-MS (Thermo Scientific, Bremen, Germany) at JAMSTEC. Samples were analyzed using the standard-sample-standard bracketing method with the AA-ETH standard (Archer et al., 2017). Specifically, three separate analyses of the same sample solution were conducted, for which uncertainties were reported as two standard deviations (2σ). The instrumental mass fractionation was corrected using Cu-doping with Cu/Zn = 1:1 (Maréchal et al., 1999). The $^{66}Zn/^{64}Zn$ ratios are expressed in delta notation relative to the JMC-LYON standard following equation (1) (Archer et al., 2017) to allow for comparison with previous studies:

$$\delta^{66}Zn_{JMC-LYON} = \left(\frac{(^{66}Zn/^{64}Zn)_{sample}}{(^{66}Zn/^{64}Zn)_{AA-ETH}} - 1 \right) \cdot 1000 + 0.28 \quad (1)$$

The repeated measurement of NIST 682 high-purity Zn as quality control yielded a $\delta^{66}Zn$ value of -2.42 ± 0.04 ‰ (n = 11, 2σ), which corresponds to values reported elsewhere (Conway et al., 2013; John et al., 2007a; John et al., 2007b). Furthermore, the accuracy of the measurements was assessed by analyzing the sediment reference

materials JLk-1 (Lake Biwa), JMS-1 (Tokyo Bay) (both provided by the Geological Survey of Japan) and MESS-4 (Beaufort Sea, Arctic Canada; provided by the National Research Council Canada), which underwent the same purification protocol as our samples. The $\delta^{66}Zn$ value of MESS-4 was $+0.26 \pm 0.04$ ‰ (n = 10) in agreement with previously reported values (Jeong et al., 2021a, 2021b). The JLk-1 reference material gave a $\delta^{66}Zn$ value of $+0.27 \pm 0.02$ ‰ (n = 6) and that of JMS-1 was $+0.29 \pm 0.04$ ‰ (n = 10).

To test for recoveries, the $\delta^{66}Zn$ value of the sum of all chemical fractions was calculated according to equation (2):

$$\delta^{66}Zn_{sum} = \left(\frac{\begin{array}{c} \delta^{66}Zn_{acid-sol\ \#1} \cdot f_{acid-sol\ \#1} + \delta^{66}Zn_{acid-sol\ \#2} \cdot f_{acid-sol\ \#2} + \\ \delta^{66}Zn_{red} \cdot f_{red} + \delta^{66}Zn_{ox} \cdot f_{ox} + \delta^{66}Zn_{res} \cdot f_{res} \end{array}}{f_{acid-sol\ \#1} + f_{acid-sol\ \#2} + f_{red} + f_{ox} + f_{res}} \right) \quad (2)$$

Here, f represents the fraction of Zn from the respective chemical fraction from the sum (acid-sol: acid-soluble; red: reducible; ox: oxidizable; res: residual).

2.8. Statistical analyses

The Pearson product-moment correlation analysis was used to explore the relationships between elemental concentrations and $\delta^{66}Zn$ values by using R version 4.3.0 (R Core Team, 2022).

3. Results and discussion

3.1. Zinc stable isotopic variations across different fractions

The Zn concentrations in the operationally defined fractions have previously been reported (Nitzsche et al., 2021, 2022), yet are summarized for the analyzed horizons (Fig. 2a and b, Table S1). In the Osaka Bay core, Zn was mostly hosted in the residual fraction (31 %–79 %), followed by the acid labile (3 %–35 %), the reducible (8 %–26 %), the oxidizable (9 %–12 %) and the exchangeable fractions (0.1 %–2 %) (Fig. 3). For Lake Biwa, Zn was mainly part of the residual fraction (61 %–84 %), followed by the reducible fraction (5 %–19 %), the oxidizable fraction (7 %–12 %), the acid-labile fraction (3 %–12 %), while almost no Zn was found in the exchangeable fraction.

The $\delta^{66}Zn$ value of the sum of fractions was usually within the analytical uncertainty (2σ) of the bulk sediments (Table S1 and Fig. S1) showing the consistency of our data. The tendency of a small enrichment in ^{66}Zn in the sum of all fractions (up to 0.06 ‰) could be explained by small sample losses during the sequential extractions leading to the underestimation of light Zn in the reducible and residual fractions. Furthermore, a complete solubility of target species is rarely possible which might lead to the transfer of Zn in one fraction to another during a later extraction step, and the unwanted solubility of other minerals. For instance, Ryan et al. (2008) observed all different extraction steps dissolved clay minerals in varying extents. We also have to point out that some phases physically protect others. For instance, Qiang et al. (1994) suggested the reduction of Fe–Mn oxyhydroxides by $NH_2OH \cdot HCl$ was hampered due to the coverage or occlusion with organic matter. Furthermore, we cannot rule out the possibility of artificial isotope fractionation caused by the used chemicals in the sequential extraction.

Using the trace metal isotopes as a fingerprinting tool requires that isotopic fractionation during early diagenesis is negligible. Organic matter oxidation by microorganisms leads to reducing conditions, which promote the reductive dissolution of Fe–Mn oxyhydroxides in subsurface sediments releasing initially bound trace metals into the porewater, which can subsequently re-adsorb to carbonates and sulphides or diffuse upward and co-precipitate with newly formed Fe–Mn oxyhydroxides (Canavan et al., 2007; Dang et al., 2015; Scholz and Neumann, 2007; Tankere-Muller et al., 2007). For Lake Biwa, the ^{210}Pb profile was not disturbed, and the pattern in Zn concentration agreed with other cores from the Lake (Nitzsche et al., 2021). Similarly, the Cu, Zn and Pb
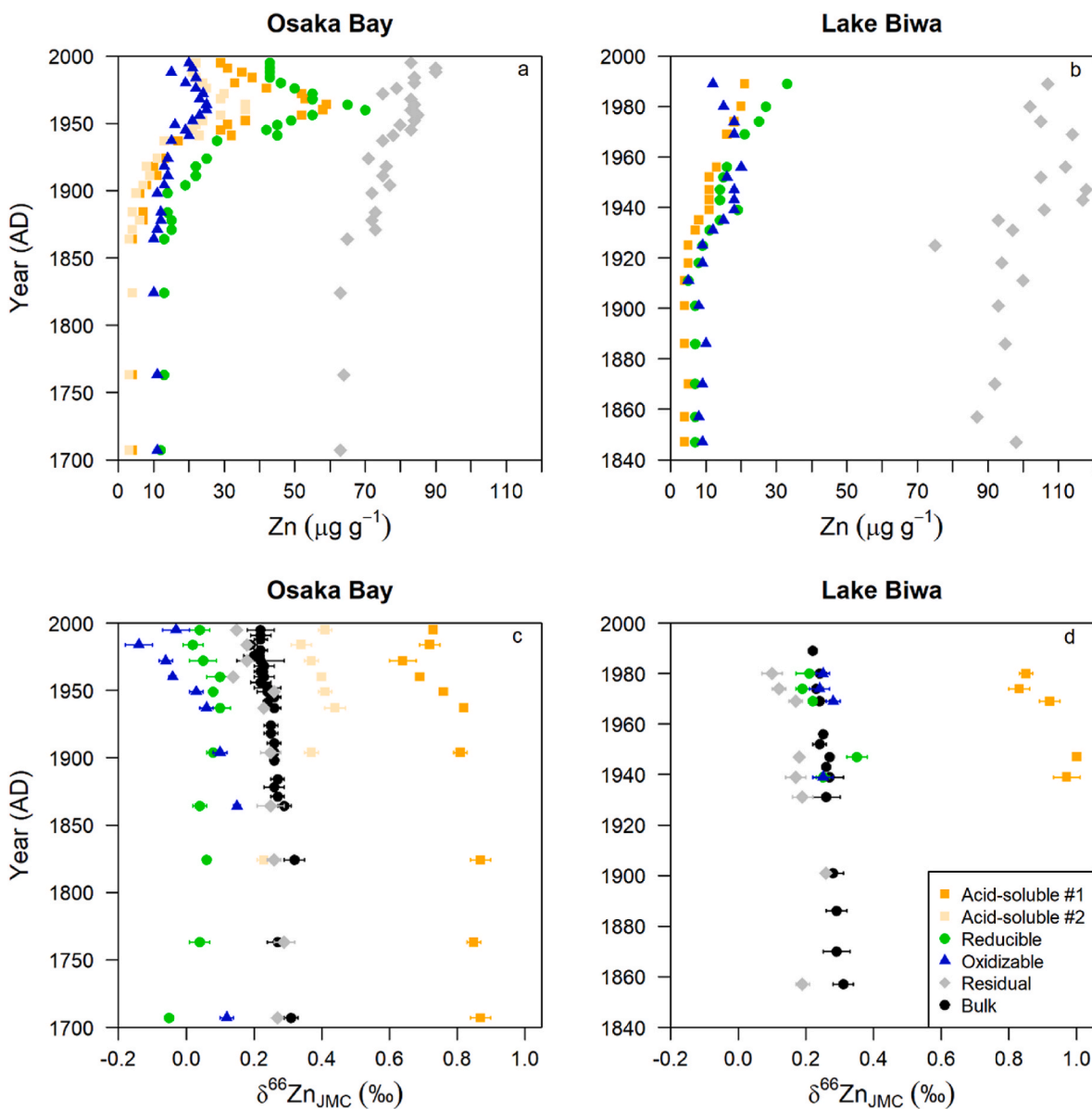
Fig. 2. Variation of Zn concentrations and $\delta^{66}Zn$ values across the operationally defined fractions for Osaka Bay (a, c) and Lake Biwa (b, d). The Zn concentrations of the operationally defined fractions (a, b) and the $\delta^{66}Zn$ values of the bulk sediments (black symbols in c, d) were taken from Nitzsche et al. (2022, 2021).

concentration patterns in the Osaka Bay core matched those in another core from Osaka Bay (Yasuhara and Yamazaki, 2005) and the trace metal patterns agreed to historical events in the catchment (Nitzsche et al., 2022). Thus, although a significant vertical movement of Zn in the sediment columns is unlikely, we cannot exclude the possibility of Zn isotopic fractionation during adsorption and precipitation processes during early diagenesis.

With respect to the Osaka Bay core, the average $\delta^{66}Zn$ value in the acid-soluble fractions #1 ($+0.73 \pm 0.03$ ‰; average ± standard error) and #2 ($+0.37 \pm 0.02$ ‰) were higher than the $\delta^{66}Zn$ values of the corresponding bulk sediments ($+0.26 \pm 0.01$ ‰) (Fig. 2c). Instead, the $\delta^{66}Zn$ values of the reducible ($+0.05 \pm 0.01$ ‰) and of the oxidizable ($+0.02 \pm 0.03$ ‰) fractions were lower than the bulk sediment, while the residual fraction ($+0.22 \pm 0.02$ ‰) was often in the range of the bulk sediment. The combined $\delta^{66}Zn$ value of the acid-soluble fraction #2 and the reducible fraction was $+0.16 \pm 0.01$ ‰ (Fig. S2). Similarly, the $\delta^{66}Zn$ value of acid-soluble fraction of Lake Biwa ($+0.91 \pm 0.03$ ‰) exceeded the bulk sediment ($+0.26 \pm 0.01$ ‰). In contrast to the Osaka Bay core, the $\delta^{66}Zn$ values of the reducible ($+0.24 \pm 0.03$ ‰) and of the oxidizable ($+0.25 \pm 0.01$ ‰) fraction in the Lake Biwa core were in the same range as the bulk sediment, while the residual fraction ($+0.17 \pm 0.01$ ‰) was lower than the bulk sediment.

Thus, the large variation in the $\delta^{66}Zn$ values across the fractions up to 0.9 ‰ within a single horizon imply different Zn sources and/or Zn isotopic fractionation during the interaction of Zn with minerals and organic matter. The enrichment in ^{66}Zn in the acid-soluble fraction #1 relative to the bulk sediment can be attributed to the preferential sorption of ^{66}Zn to carbonates ($\delta^{66}Zn_{adsorbed}$ - $\delta^{66}Zn_{solution} = \Delta^{66}Zn_{adsorbed-solution} = +0.73 \pm 0.08$ ‰; at high ionic strength) (Dong and Wasylenki, 2016) and/or the preferential incorporation of ^{66}Zn into calcite ($\Delta^{66}Zn_{calcite-solution} = +0.58 \pm 0.05$ ‰) (Mavromatis et al., 2019). Calcite was identified in traces (<1 %) in the Osaka Bay core (Table 2). Carbonates have likely derived from calcific foraminifera and ostracods in the water column (Tsujimoto et al., 2006; Yasuhara and Yamazaki, 2005) which could incorporate Zn into their shells. The lower $\delta^{66}Zn$ values of the acid-soluble #2 fraction extracted from the Osaka Bay core could indicate the extraction of more refractory carbonate pool dominated by aragonite, which shows a lower extractability with acetic acid
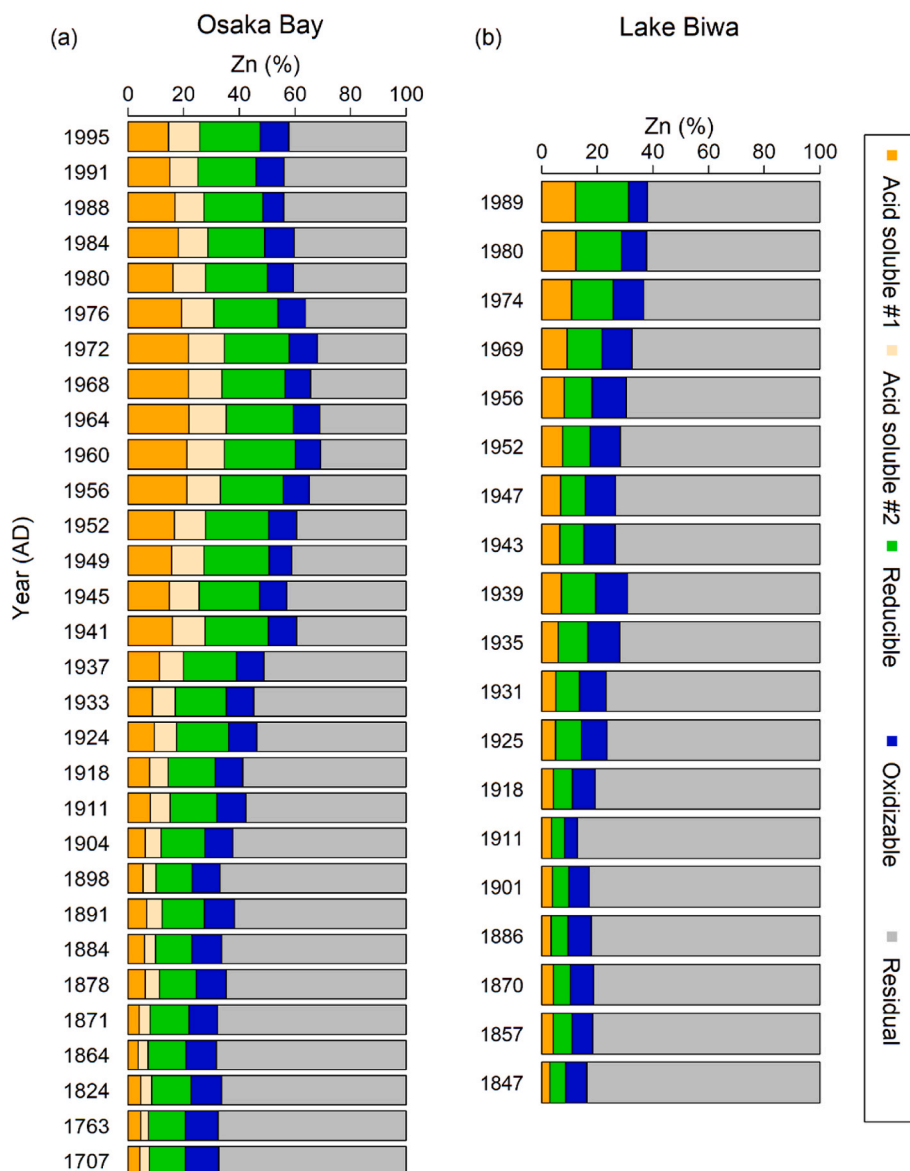
Fig. 3. Distribution of Zn in the operationally defined fractions (expressed in % of the sum of all fractions) for Osaka Bay (a) and Lake Biwa (b). The Zn concentrations of the operationally defined fractions were taken from Nitzsche et al. (2022, 2021).

Table 2
Mineral assemblage of the selected samples from the Osaka and Lake Biwa cores determined by XRD analysis.

Core	Year (AD)	Cal	Chl	Ill	Pl	Qtz
Osaka Bay	1995	o	x	xx	xx	xx
Osaka Bay	1972	o	x	xx	xx	xx
Osaka Bay	1960	o	xx	xx	xx	xx
Osaka Bay	1937	o	xx	xx	xx	xx
Osaka Bay	1904	o	xx	xx	xxx	xx
Osaka Bay	1763	o	xx	xx	xx	xx
Lake Biwa	1989		x	xx	xx	xxx
Lake Biwa	1969		xx	xx	x	xxx
Lake Biwa	1956		xx	xx	x	xxx
Lake Biwa	1931		xx	xx	x	xxx
Lake Biwa	1911		xx	xx	x	xxx
Lake Biwa	1847		xx	xx	x	xx

Abbreviations: Cal, calcite; Chl, chlorite; Ill, illite; Pl, plagioclase; Qtz, quartz.
xxx = abundant; xx = common; x = minor; o = trace.

compared to calcite (Ryu et al., 2010). Higher molar Sr/Ca and Ba/Ca ratios in the acid-soluble #2 fraction support the presence of aragonite (Fig. S3) (Rosenheim et al., 2005). Such aragonite could have derived from mollusks present in Osaka Bay. It was shown that aragonite minerals fractionate Zn isotopes to a lesser extent than calcite minerals (Zhao et al., 2021).

Zinc in the reducible fraction was associated with Mn rather than with Fe oxyhydroxides owing to stronger correlations of Mn with Zn (Fig. 4). In fact, Fe (hydr)oxides such as hematite and magnetite were not identified by XRD analysis (Table 2). However, short-range order Mn and Fe oxyhydroxides such as birnessite and ferrihydrite cannot be accurately identified by XRD analysis. The Zn isotopic fractionation during the sorption to different Fe–Mn oxyhydroxides including birnessite, ferrihydrite and goethite is complex and depends on ionic strength, pH, exposure time and surface coverage (Balistrieri et al., 2008; Bryan et al., 2015; Juillot et al., 2008; Komárek et al., 2022; Pokrovsky et al., 2005; Wang et al., 2023; Yan et al., 2023). Yet, we cannot exclude that carbonates enriched in ^{66}Zn were not fully dissolved during the extraction with acetic acid leading to higher values in the reducible fraction of Lake Biwa. The similar δ^{66}Zn values in the
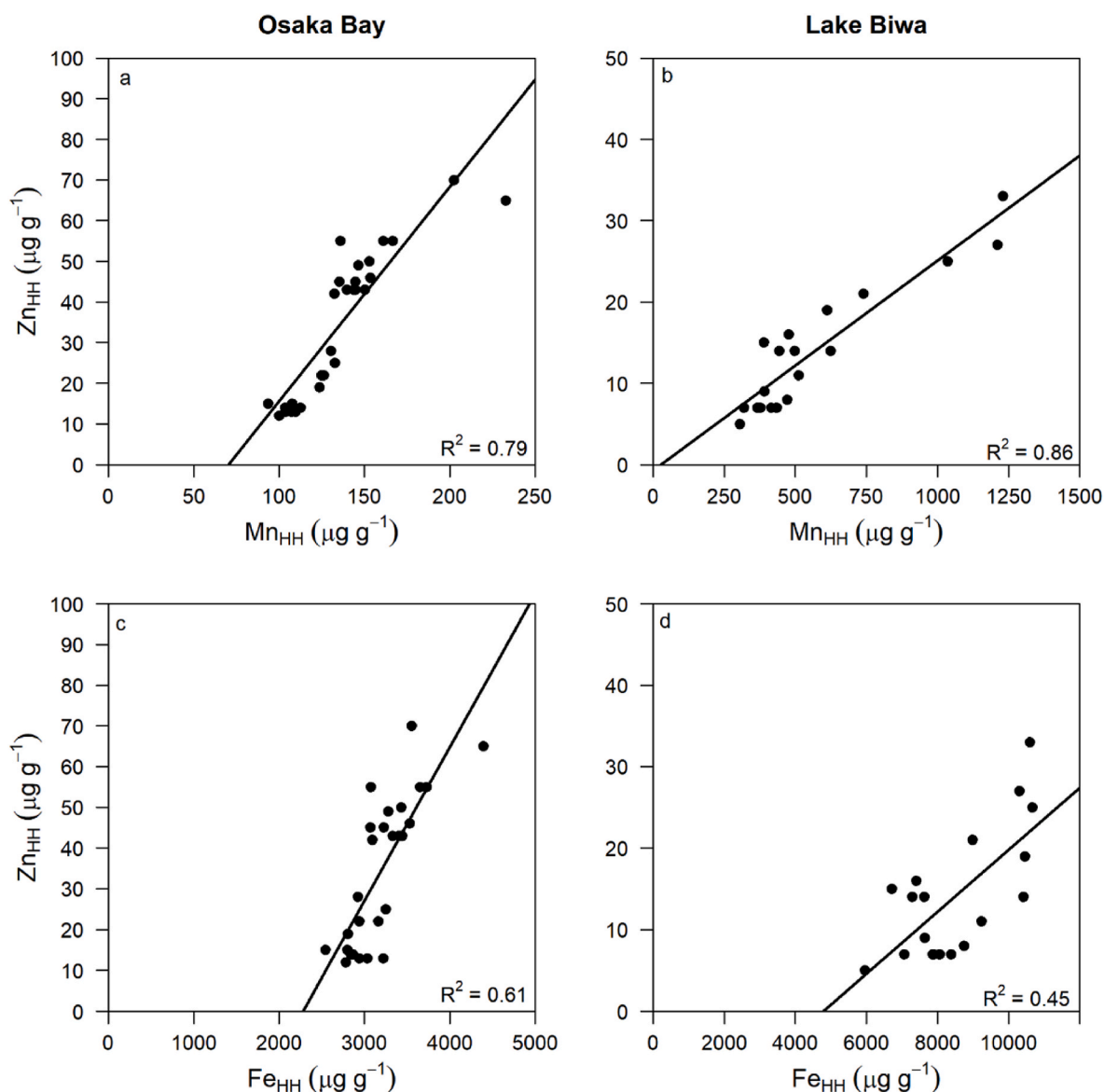
Fig. 4. Scatter plot of Zn against Mn and Fe extracted by hydroxylamine hydrochloride (HH) for Osaka Bay (a, c) and for Lake Biwa (b, d).

reducible fraction and in the bulk sediment of Lake Biwa agree with the negligible Zn isotope fractionation ($\Delta^{66}Zn_{solid-solution} = +0.05 \pm 0.08$ ‰) to birnessite at low ionic strength (<0.001 M) (Bryan et al., 2015). However, the depletion of ^{66}Zn in the reducible fraction of the Osaka Bay core is in contrast to the ^{66}Zn enrichment ($+0.16$ to $+2.74$ ‰ with decreasing surface coverage) at high ionic strength (0.7 M, artificial seawater) on birnessite (Bryan et al., 2015). A recent adsorption experiment using birnessite determined $\Delta^{66}Zn_{solid-solution}$ as -0.46 ± 0.04 ‰ at pH 3–5 and at low Zn/Mn molar ratios (0.0370–0.170), which decreased to -0.09 ± 0.05 ‰ at pH 6–8 at high Zn/Mn molar ratios (0.170–0.327) (Wang et al., 2023). In contrast to adsorption, the substitution of Zn into crystal lattices of goethite was shown to prefer the light Zn isotopes ($\Delta^{66}Zn_{substituted-solution} = -1.52 \pm 0.09$ ‰, pH 8.0) (Yan et al., 2023). Such incorporation of Zn in crystals represents a less recognized Zn isotopic fractionation mechanism compared to sorption. We hypothesize that the lower $\delta^{66}Zn$ in the reducible fraction of the Osaka Bay core could be explained by a combination of Zn isotope fractionation during sorption of Zn to and possible incorporation into Fe–Mn oxyhydroxides such as birnessite and ferrihydrite. A depletion in ^{66}Zn was also found in a fraction extracted with 5M HCl, which was assumed to target at Fe oxides in sediment core from an urban lake

(Thapalia et al., 2010). Yet, Zn could also be derived from crystal lattices of clay minerals such as smectite, which are partly dissolved in HCl (Yoshimura et al., 2023). Although it was suggested that low $\delta^{66}Zn$ values in the reducible fraction extracted with 5M HCl were due to the adsorption of anthropogenic Zn depleted in ^{66}Zn (Thapalia et al., 2010), a preferential incorporation of ^{64}Zn into Fe oxides also sounds plausible. Consequently, it is clear that Zn isotopic fractionation strongly differs between laboratory and natural conditions with the latter further differing depending on the system (lacustrine vs. marine).

The low $\delta^{66}Zn$ values in the oxidizable fraction (-0.14 to $+0.12$ ‰) of the Osaka Bay core are well in agreement with the low $\delta^{66}Zn$ values observed for organic-rich continental sediments from the east Pacific margins (Little et al., 2016). Such depletion in ^{66}Zn is likely due to the preferential incorporation of ^{64}Zn ($\Delta^{66}Zn_{solid-solution} = -0.8$ to -0.2 ‰) into phytoplankton (John et al., 2007a). The negative correlation between $\delta^{66}Zn$ in the oxidizable fraction and the TOC concentrations supports this assumption (Fig. 5). In contrast, the higher $\delta^{66}Zn$ values in the oxidizable fraction of the Lake Biwa core ($+0.24$ to $+0.28$ ‰) could indicate the contribution of dissolved and suspended particulate matter enriched in ^{66}Zn and/or a species-dependent stronger ^{66}Zn enrichment in freshwater compared to marine phytoplankton. In fact, the higher
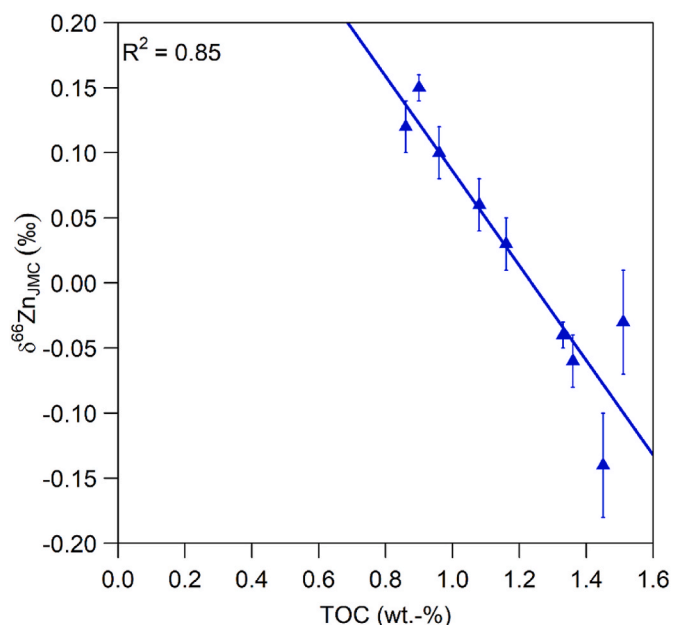
Fig. 5. Satter plot of δ^{66}Zn in the oxidizable fraction against the total organic carbon (TOC) content in the sediment core from Osaka Bay.

δ^{66}Zn values in the oxidizable fraction of the Lake Biwa core are consistent with the estimate of +0.33 ‰ of rivers globally (Little et al., 2014).

Lastly, the average δ^{66}Zn value of the residual fraction of the Osaka Bay core (+0.22 ± 0.02 ‰) was close to the average δ^{66}Zn value of silicate rocks which is around +0.28 ± 0.05 ‰ (Chen et al., 2013). Slightly lower values in the upper part of the core (>1950 AD) could be due to the incomplete dissolution of Fe–Mn oxyhydroxides and the incomplete oxidation of organic matter. Yet, the presence of such phases depleted in ^{66}Zn cannot explain the lower δ^{66}Zn values in the residual fraction of the Lake Biwa core (+0.17 ± 0.01 ‰) because the δ^{66}Zn values in the reducible and oxidizable fractions were close to the bulk sediment. At the moment, we lack an explanation for such low δ^{66}Zn values in the upper part of the Lake Biwa core. Future studies may target at the Zn stable isotope composition in the crystal lattice of individual minerals such as feldspars and clay minerals. For instance, chlorite is common in all samples (Table 2) and could be depleted in ^{66}Zn.

3.2. Anthropogenic impacts on Zn stable isotopes in single fractions

Slight decreases in the δ^{66}Zn values of the bulk sediments from the 1950s in the Osaka Bay and Lake Biwa cores indicated the contribution of an urban, industrial Zn source depleted in ^{66}Zn (+0.14 ‰ for Lake Biwa and +0.17 ‰ for Osaka Bay, respectively), which was estimated assuming a two-endmember mixing model (Nitzsche et al., 2021, 2022). Typical δ^{66}Zn values of urban, industrial sources are tire wear (+0.08 to +0.21 ‰) and road dust (+0.08 to +0.17 ‰) (Dong et al., 2017; Sou-to-Oliveira et al., 2018; Thapalia et al., 2010), industrial effluents (+0.10 to +0.15 ‰) (Desaulty and Petelet-Giraud, 2020), and effluents from wastewater treatment plants (−0.03 to +0.11 ‰) (Chen et al., 2008; Desaulty and Petelet-Giraud, 2020; Sakata et al., 2019). Furthermore, the contribution of effluents from electroplating plants enriched in ^{66}Zn (up to +3.5 ‰) (Kavner et al., 2008) was suspected for the Osaka Bay core (Nitzsche et al., 2022). However, the δ^{66}Zn values of the bulk sediments neither reflected the increasing Zn concentrations from the 1870s, nor the decreasing Zn concentrations after the peak in the 1960s in the Osaka Bay core (Figs. 2 and 3) indicating that the δ^{66}Zn values of the natural and anthropogenic endmembers were similar during these times and/or that further sources and transformations with

isotopic fractionation existed. For instance, despite the increase in the Zn concentration of the reducible fraction towards the surface, which accounted for 6–26 % of the total Zn (Fig. 2a and 3a; Nitzsche et al., 2022), the corresponding δ^{66}Zn values showed no clear pattern and scattered from −0.05 to +0.10 ‰ (Fig. 2c–Table S1). This scatter can be attributed to the complicated fractionation of Zn stable isotopes during the adsorption to and incorporation into Fe–Mn oxyhydroxides at high ionic strength (Balistrieri et al., 2008; Bryan et al., 2015; Juillot et al., 2008; Pokrovsky et al., 2005; Yan et al., 2023).

The δ^{66}Zn values in the acid-soluble fraction #1 and oxidizable fraction tended to decrease from around 1900 AD, decreased more strongly from the 1950s (also the residual fraction), being lowest in the early 1970s (acid-soluble fraction #1) and 1980s (oxidizable fractions), from when the δ^{66}Zn values increased again (Fig. 2c). Such pattern is more consistent with the corresponding Zn concentrations (Fig. 2a). Consequently, stronger correlations were observed between δ^{66}Zn values and the Zn concentrations in the acid-soluble fraction #1 and oxidizable fraction compared to the bulk sediment (Fig. 6a). Although some data points are missing, such stronger correlations indicate that the acid-soluble fraction #1 and oxidizable fraction could be more susceptible to changes in Zn sources than the corresponding bulk sediment. For Lake Biwa, a decrease in the δ^{66}Zn values was observed in the residual, reducible and acid-soluble fractions from the 1960s indicating the contribution of anthropogenic Zn depleted in ^{66}Zn (Fig. 2d). Yet, estimating the δ^{66}Zn values of the anthropogenic endmember(s) are challenging 1) due to the missing Δ^{66}Zn$_{\text{solid-solution}}$ values for the different fractions and 2) because more than two Zn sources could exist depending on the fraction. The better agreement of the δ^{66}Zn values of the reducible fraction of Lake Biwa compared to the reducible fraction of Osaka Bay could be related to the lower ionic strength in Lake Biwa, which might cause less Zn isotope fractionation. Instead, temporal changes in Zn from particulate and dissolved inputs could explain why the δ^{66}Zn values of the oxidizable fraction of Lake Biwa are not in a good agreement with the corresponding Zn concentrations.

4. Conclusions

The large variation of approximately 0.9 ‰ in δ^{66}Zn values across the operationally defined fractions strongly exceeded the difference in the δ^{66}Zn values of the natural (~0.28 ± 0.02 ‰) and of the anthropogenic endmember (~0.15 ± 0.02 ‰) which was estimated for the Osaka Bay and Lake Biwa cores when using a binary mixing model (Nitzsche et al., 2021, 2022). Thus, Zn isotopic fractionation during the sorption to minerals (e.g. Fe–Mn oxyhydroxides) and organic matter in the water and in the sediment column and during co-precipitation, the latter as a result of diagenetic alteration, must be considered when using trace metal isotopes of bulk sediments as a fingerprinting tool for anthropogenic contamination (Komárek et al., 2022). For Osaka Bay, the δ^{66}Zn values of the acid-soluble fraction #1 and oxidizable fraction, and for Lake Biwa, the δ^{66}Zn values of the acid-soluble and oxidizable fractions better reflected the temporal change in the Zn concentration than the bulk sediment indicating that these fractions could be a sensitive fingerprinting tool for anthropogenic Zn contamination rather than the bulk sediment. Yet, isotopic fractionation needs to be precisely determined to demonstrate their potential usage to reliably estimating the δ^{66}Zn values of the anthropogenic endmember(s). Furthermore, the environmental conditions (e.g. ionic strength) and phytoplankton species likely drive the Zn isotopic systematics in the reducible and oxidizable fractions. Thus, the coupling of Zn stable isotopes with sequential extraction represents a promising tool for assessing the preferential binding of anthropogenic Zn while considering Zn isotope fractionation during the sorption of Zn. Further studies on the trace metal isotopic composition of operationally defined fractions, which ideally also account for isotopic fractionation during diagenesis, are required. In this regard, knowing the δ^{66}Zn value of the dissolved Zn sources in the water column as well as in the porewater is crucial to

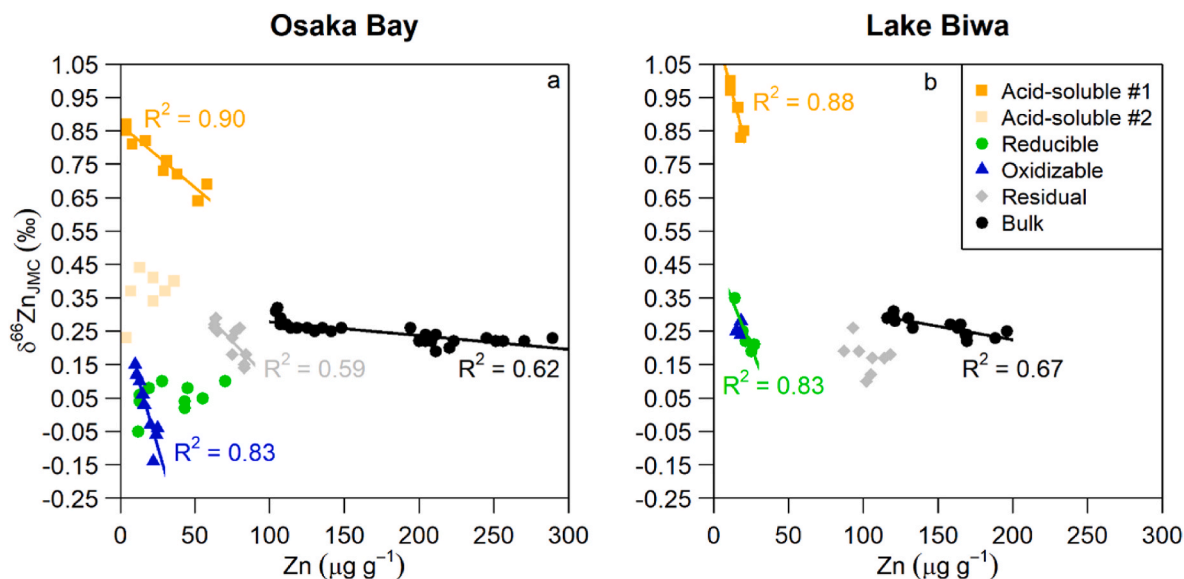**Fig. 6.** Scatter plot of $\delta^{66}Zn$ against the Zn concentrations in the bulk sediments and different chemical fractions in the core from Osaka Bay (a) and in the core from Lake Biwa (b).

accounting for such diagenetic impacts.

CRediT authorship contribution statement

Kai Nils Nitzsche: Writing – review & editing, Writing – original draft, Methodology, Investigation, Data curation, Conceptualization. **Toshihiro Yoshimura:** Writing – review & editing, Supervision, Resources, Methodology, Conceptualization. **Naoto F. Ishikawa:** Writing – review & editing, Supervision. **Hodaka Kawahata:** Writing – review & editing, Conceptualization. **Nanako O. Ogawa:** Writing – review & editing, Methodology, Data curation. **Katsuhiko Suzuki:** Writing – review & editing, Methodology. **Daisuke Araoka:** Writing – review & editing, Methodology, Data curation. **Naohiko Ohkouchi:** Writing – review & editing, Supervision.

Declaration of competing interest

The authors declare that they have no known competing financial interests or personal relationships that could have appeared to influence the work reported in this paper.

Data availability

Data will be made available on request.

Appendix A. Supplementary data

Supplementary data to this article can be found online at https://doi.org/10.1016/j.apgeochem.2024.106047.

References

Araoka, D., Simandl, G.J., Paradis, S., Yoshimura, T., Hoshino, M., Kon, Y., 2022. Formation of the Rock Canyon Creek carbonate-hosted REE–F–Ba deposit, British Columbia, Canada: constraints from Mg-Sr isotopes of dolomite, calcite, and fluorite. J. Geochem. Explor. 240, 107045 https://doi.org/10.1016/j.gexplo.2022.107045.

Araújo, D.F., Boaventura, G.R., Machado, W., Viers, J., Weiss, D., Patchineelam, S.R., Ruiz, I., Rodrigues, A.P.C., Babinski, M., Dantas, E., 2017. Tracing of anthropogenic zinc sources in coastal environments using stable isotope composition. Chem. Geol. 449, 226–235. https://doi.org/10.1016/j.chemgeo.2016.12.004.

Araújo, D.F., Knoery, J., Briant, N., Vigier, N., Ponzevera, E., 2022. "Non-traditional" stable isotopes applied to the study of trace metal contaminants in anthropized marine environments. Mar. Pollut. Bull. 175, 113398 https://doi.org/10.1016/j.marpolbul.2022.113398.

Araújo, D.F., Ponzevera, E., Briant, N., Knoery, J., Sireau, T., Mojtahid, M., Metzger, E., Brach-Papa, C., 2019. Assessment of the metal contamination evolution in the Loire estuary using Cu and Zn stable isotopes and geochemical data in sediments. Mar. Pollut. Bull. 143, 12–23. https://doi.org/10.1016/j.marpolbul.2019.04.034.

Archer, C., Andersen, M.B., Cloquet, C., Conway, T.M., Dong, S., Ellwood, M., Moore, R., Nelson, J., Rehkämper, M., Rouxel, O., Samanta, M., Shin, K.C., Sohrin, Y., Takano, S., Wasylenki, L., 2017. Inter-calibration of a proposed new primary reference standard AA-ETH Zn for zinc isotopic analysis. J. Anal. At. Spectrom. 32, 415–419. https://doi.org/10.1039/c6ja00282j.

Bacon, J.R., Davidson, C.M., 2008. Is there a future for sequential chemical extraction? Analyst 133, 25–46. https://doi.org/10.1039/b711896a.

Balistrieri, L.S., Borrok, D.M., Wanty, R.B., Ridley, W.I., 2008. Fractionation of Cu and Zn isotopes during adsorption onto amorphous Fe(III) oxyhydroxide: experimental mixing of acid rock drainage and ambient river water. Geochem. Cosmochim. Acta 72, 311–328. https://doi.org/10.1016/j.gca.2007.11.013.

Bigalke, M., Weyer, S., Kobza, J., Wilcke, W., 2010. Stable Cu and Zn isotope ratios as tracers of sources and transport of Cu and Zn in contaminated soil. Geochem. Cosmochim. Acta 74, 6801–6813. https://doi.org/10.1016/j.gca.2010.08.044.

Bronk Ramsey, C., 2009. Bayesian analysis of radiocarbon dates. Radiocarbon 51, 337–360. https://doi.org/10.1017/s0033822200033865.

Bryan, A.L., Dong, S., Wilkes, E.B., Wasylenki, L.E., 2015. Zinc isotope fractionation during adsorption onto Mn oxyhydroxide at low and high ionic strength. Geochem. Cosmochim. Acta 157, 182–197. https://doi.org/10.1016/j.gca.2015.01.026.

Canavan, R.W., van Cappellen, P., Zwolsman, J.J.G., van den Berg, G.A., Slomp, C.P., 2007. Geochemistry of trace metals in a fresh water sediment: field results and diagenetic modeling. Sci. Total Environ. 381, 263–279. https://doi.org/10.1016/j.scitotenv.2007.04.001.

Chen, H., Savage, P.S., Teng, F.Z., Helz, R.T., Moynier, F., 2013. Zinc isotope fractionation during magmatic differentiation and the isotopic composition of the bulk Earth. Earth Planet Sci. Lett. 369–370, 34–42. https://doi.org/10.1016/j.epsl.2013.02.037.

Chen, J., Gaillardet, J., Louvat, P., 2008. Zinc isotopes in the Seine River waters, France: a probe of anthropogenic contamination. Environ. Sci. Technol. 42, 6494–6501. https://doi.org/10.1021/es800725z.

Conway, T.M., Rosenberg, A.D., Adkins, J.F., John, S.G., 2013. A new method for precise determination of iron, zinc and cadmium stable isotope ratios in seawater by double-spike mass spectrometry. Anal. Chim. Acta 793, 44–52. https://doi.org/10.1016/j.aca.2013.07.025.

Dang, D.H., Lenoble, V., Durrieu, G., Omanović, D., Mullot, J.U., Mounier, S., Garnier, C., 2015. Seasonal variations of coastal sedimentary trace metals cycling: insight on the

effect of manganese and iron (oxy)hydroxides, sulphide and organic matter. Mar. Pollut. Bull. 92, 113–124. https://doi.org/10.1016/j.marpolbul.2014.12.048.

Desaulty, A.M., Petelet-Giraud, E., 2020. Zinc isotope composition as a tool for tracing sources and fate of metal contaminants in rivers. Sci. Total Environ. 728, 138599 https://doi.org/10.1016/j.scitotenv.2020.138599.

Dong, S., Ochoa Gonzalez, R., Harrison, R.M., Green, D., North, R., Fowler, G., Weiss, D., 2017. Isotopic signatures suggest important contributions from recycled gasoline, road dust and non-exhaust traffic sources for copper, zinc and lead in PM10 in London, United Kingdom. Atmos. Environ. 165, 88–98. https://doi.org/10.1016/j.atmosenv.2017.06.020.

Dong, S., Wasylenki, L.E., 2016. Zinc isotope fractionation during adsorption to calcite at high and low ionic strength. Chem. Geol. 447, 70–78. https://doi.org/10.1016/j.chemgeo.2016.10.031.

Gao, C., Yu, J., Min, X., Cheng, A., Hong, R., Zhang, L., 2018. Heavy metal concentrations in sediments from Xingyun lake, southwestern China: implications for environmental changes and human activities. Environ. Earth Sci. 77, 1–13. https://doi.org/10.1007/s12665-018-7840-5.

Gélabert, A., Pokrovsky, O.S., Viers, J., Schott, J., Boudou, A., Feurtet-Mazel, A., 2006. Interaction between zinc and freshwater and marine diatom species: surface complexation and Zn isotope fractionation. Geochem. Cosmochim. Acta 70, 839–857. https://doi.org/10.1016/j.gca.2005.10.026.

Hass, A., Fine, P., 2010. Sequential selective extraction procedures for the study of heavy metals in soils, sediments, and waste materials—a critical review. Crit. Rev. Environ. Sci. Technol. 40, 365–399. https://doi.org/10.1080/10643380802377992.

Heaton, T.J., Köhler, P., Butzin, M., Bard, E., Reimer, R.W., Austin, W.E.N., Bronk Ramsey, C., Grootes, P.M., Hughen, K.A., Kromer, B., Reimer, P.J., Adkins, J., Burke, A., Cook, M.S., Olsen, J., Skinner, L.C., 2020. Marine20 - the marine radiocarbon age calibration curve (0-55,000 cal BP). Radiocarbon 62, 779–820. https://doi.org/10.1017/RDC.2020.68.

Hornberger, M.I., Luoma, S.N., Van Geen, A., Fuller, C., Anima, R., 1999. Historical trends of metals in the sediments of San Francisco Bay, California. Mar. Chem. 64, 39–55. https://doi.org/10.1016/S0304-4203(98)80083-2.

Itihara, M., Yoshikawa, S., Kamei, T., Nasu, T., 1988. Stratigraphic subdivision of quaternary deposits in Kinki District, Japan. Mem. Geol. Soc. Japan 30, 111–125 (In Japanese).

Jeong, H., Lee, Y., Moon, H.B., Ra, K., 2023. Characteristics of metal pollution and multi-isotopic signatures for C, Cu, Zn, and Pb in coastal sediments from special management areas in Korea. Mar. Pollut. Bull. 188, 114642 https://doi.org/10.1016/j.marpolbul.2023.114642.

Jeong, H., Ra, K., Choi, J.Y., 2021a. Copper, zinc and lead isotopic delta values and isotope ratios of various geological and biological reference materials. Geostand. Geoanal. Res. 45, 551–563. https://doi.org/10.1111/ggr.12379.

Jeong, H., Ra, K., Won, J.H., 2021b. A nationwide survey of trace metals and Zn isotopic signatures in mussels (Mytilus edulis) and oysters (Crassostrea gigas) from the coast of South Korea. Mar. Pollut. Bull. 173, 113061 https://doi.org/10.1016/j.marpolbul.2021.113061.

John, S.G., Geis, R.W., Saito, M.A., Boyle, E.A., 2007b. Zinc isotope fractionation and low-affinity zinc transport during by the marine diatom Thalassiosira oceanica. Limnology 52, 2710–2714. https://doi.org/10.4319/lo.2007.52.6.2710.

John, S.G., Genevieve Park, J., Zhang, Z., Boyle, E.A., 2007a. The isotopic composition of some common forms of anthropogenic zinc. Chem. Geol. 245, 61–69. https://doi.org/10.1016/j.chemgeo.2007.07.024.

Juillot, F., Maréchal, C., Ponthieu, M., Cacaly, S., Morin, G., Benedetti, M., Hazemann, J. L., Proux, O., Guyot, F., 2008. Zn isotopic fractionation caused by sorption on goethite and 2-Lines ferrihydrate. Geochem. Cosmochim. Acta 72, 4886–4900. https://doi.org/10.1016/j.gca.2008.07.007.

Kavner, A., John, S.G., Sass, S., Boyle, E.A., 2008. Redox-driven stable isotope fractionation in transition metals: application to Zn electroplating. Geochem. Cosmochim. Acta 72, 1731–1741. https://doi.org/10.1016/j.gca.2008.01.023.

Komárek, M., Ratié, G., Vaňková, Z., Šípková, A., Chrastný, V., 2022. Metal isotope complexation with environmentally relevant surfaces - opening the isotope fractionation black box. Crit. Rev. Environ. Sci. Technol. 52, 3573–3603. https://doi.org/10.1080/10643389.2021.1955601.

Kuwae, M., Yamamoto, M., Ikehara, K., Irino, T., Takemura, K., Sagawa, T., Sakamoto, T., Ikehara, M., Takeoka, H., 2013. Stratigraphy and wiggle-matching-based age-depth model of late Holocene marine sediments in Beppu Bay, southwest Japan. J. Asian Earth Sci. 69, 133–148. https://doi.org/10.1016/j.jseaes.2012.07.002.

Little, S.H., Vance, D., McManus, J., Severmann, S., 2016. Key role of continental margin sediments in the oceanic mass balance of Zn and Zn isotopes. Geology 44, 207–210. https://doi.org/10.1130/G37493.1.

Little, S.H., Vance, D., Walker-Brown, C., Landing, W.M., 2014. The oceanic mass balance of copper and zinc isotopes, investigated by analysis of their inputs, and outputs to ferromanganese oxide sediments. Geochem. Cosmochim. Acta 125, 673–693. https://doi.org/10.1016/j.gca.2013.07.046.

Maréchal, C.N., Télouk, P., Albarède, F., 1999. Precise analysis of copper and zinc isotopic compositions by plasma-source mass spectrometry. Chem. Geol. 156, 251–273. https://doi.org/10.1016/S0009-2541(98)00191-0.

Matsuzaki, H., Nakano, C., Yamashita, H., Maejima, Y., Miyairi, Y., Wakasa, S., Horiuchi, K., 2004. Current status and future direction of MALT, the University of Tokyo. Nucl. Instrum. Methods Phys. Res. Sect. B Beam Interact. Mater. Atoms 223–224, 92–99. https://doi.org/10.1016/j.nimb.2004.04.022.

Mavromatis, V., Gonzáleza, A.G., Dietzel, M., Schott, J., 2019. Zinc isotope fractionation during the inorganic precipitation of calcite – towards a new pH proxy. Geochem. Cosmochim. Acta 244, 99–112. https://doi.org/10.1016/j.gca.2018.09.005.

Miyoshi, Y., Ishibashi, J. Ichiro, Shimada, K., Inoue, H., Uehara, S., Tsukimura, K., 2015. Clay minerals in an active hydrothermal field at Iheya-North-Knoll, Okinawa trough. Resour. Geol. 65, 346–360. https://doi.org/10.1111/rge.12078.

Müsing, K., Clarkson, M.O., Vance, D., 2022. The meaning of carbonate Zn isotope records: constraints from a detailed geochemical and isotope study of bulk deep-sea carbonates. Geochem. Cosmochim. Acta 324, 26–43. https://doi.org/10.1016/j.gca.2022.02.029.

Nelson, J., Wasylenki, L., Bargar, J.R., Brown Jr, G.E., Maher, K., 2017. Effects of surface structural disorder and surface coverage on isotopic fractionation during Zn(II) adsorption onto quartz and amorphous silica surfaces. Geochem. Cosmochim. Acta 215, 354–376. https://doi.org/10.1016/j.gca.2017.08.003.

Nitzsche, K.N., Yoshimura, T., Ishikawa, N.F., Kajita, H., Kawahata, H., Ogawa, N.O., Suzuki, K., Yokoyama, Y., Ohkouchi, N., 2022. Metal contamination in a sediment core from Osaka Bay during the last 400 years. Prog. Earth Planet. Sci. 9, 58. https://doi.org/10.1186/s40645-022-00517-z.

Nitzsche, K.N., Yoshimura, T., Ishikawa, N.F., Ogawa, N.O., Suzuki, K., Ohkouchi, N., 2021. Trace metal geochemical and Zn stable isotope data as tracers for anthropogenic metal contributions in a sediment core from Lake Biwa, Japan. Appl. Geochem. 134, 105107 https://doi.org/10.1016/j.apgeochem.2021.105107.

Ogawa, N.O., Koitabashi, T., Oda, H., Nakamura, T., Ohkouchi, N., Wada, E., 2001. Fluctuations of nitrogen isotope ratio of gobiid fish (Isaza) specimens and sediments in Lake Biwa, Japan, during the 20th century. Limnol. Oceanogr. 46, 1228–1236. https://doi.org/10.4319/lo.2001.46.5.1228.

Ogawa, N.O., Nagata, T., Kitazato, H., Ohkouchi, N., 2010. Ultra-sensitive elemental analyzer/isotope ratio mass spectrometer for stable nitrogen and carbon isotope analyses. In: Ohkouchi, N., Tayasu, I., Koba, K. (Eds.), Earth, Life, and Isotopes. Kyoto University Press, pp. 339–353.

Petts, G.E., 1988. Water management: the case of Lake Biwa, Japan. Geogr. J. 154, 367–376. https://doi.org/10.2307/634609.

Pokrovsky, O.S., Viers, J., Freydier, R., 2005. Zinc stable isotope fractionation during its adsorption on oxides and hydroxides. J. Colloid Interface Sci. 291, 192–200. https://doi.org/10.1016/j.jcis.2005.04.079.

Qiang, T., Xiao-quan, S., Zhe-ming, N., 1994. Evaluation of a sequential extraction procedure for the fractionation of amorphous iron and manganese oxides and organic matter in soils. Sci. Total Environ. 151, 159–165. https://doi.org/10.1016/0048-9697(94)90172-4.

R Core Team, 2022. R: A Language and Environment for Statistical Computing. R Foundation for Statistical Computing, Vienna, Austria. URL. https://www.R-project.org/.

Rauret, G., López-Sánchez, J.F., Sahuquillo, A., Rubio, R., Davidson, C., Ure, A., Quevauviller, P., 1999. Improvement of the BCR three step sequential extraction procedure prior to the certification of new sediment and soil reference materials. J. Environ. Monit. 1, 57–61. https://doi.org/10.1039/a807854h.

Rosenheim, B.E., Swart, P.K., Thorrold, S.R., 2005. Minor and trace elements in sclerosponge Ceratoporella nicholsoni: biogenic aragonite near the inorganic endmember? Palaeogeogr. Palaeoclimatol. Palaeoecol. 228, 109–129. https://doi.org/10.1016/j.palaeo.2005.03.055.

Ryan, P.C., Hillier, S., Wall, A.J., 2008. Stepwise effects of the BCR sequential chemical extraction procedure on dissolution and metal release from common ferromagnesian clay minerals: a combined solution chemistry and X-ray powder diffraction study. Sci. Total Environ. 407, 603–614. https://doi.org/10.1016/j.scitotenv.2008.09.019.

Ryu, H., Kim, H., Lim, M., You, K., Ahn, J., 2010. Comparison of dissolution and surface reactions between calcite and aragonite in L-glutamic and L-aspartic acid solutions. Molecules 15, 258–269. https://doi.org/10.3390/molecules15010258.

Sahuquillo, A., López-Sánchez, J.F., Rubio, R., Rauret, G., Thomas, R.P., Davidson, C.M., Ure, A.M., 1999. Use of a certified reference material for extractable trace metals to assess sources of uncertainty in the BCR three-stage sequential extraction procedure. Anal. Chim. Acta 382, 317–327. https://doi.org/10.1016/S0003-2670(98)00754-5.

Sakata, M., Okuizumi, S., Mashio, A.S., Ohno, T., Sakata, S., 2019. Evaluation of pollution sources of zinc in Tokyo Bay based on zinc isotope ratio in sediment core. J. Geosci. Environ. Protect. 7, 141–154. https://doi.org/10.4236/gep.2019.78010.

Scholz, F., Neumann, T., 2007. Trace element diagenesis in pyrite-rich sediments of the Achterwasser lagoon, SW Baltic Sea. Mar. Chem. 107, 516–532. https://doi.org/10.1016/j.marchem.2007.08.005.

Sossi, P.A., Halverson, G.P., Nebel, O., Eggins, S.M., 2015. Combined separation of Cu, Fe and Zn from rock matrices and improved analytical protocols for stable isotope determination. Geostand. Geoanal. Res. 39, 129–149. https://doi.org/10.1111/j.1751-908X.2014.00298.x.

Souto-Oliveira, C.E., Babinski, M., Araújo, D.F., Andrade, M.F., 2018. Multi-isotopic fingerprints (Pb, Zn, Cu) applied for urban aerosol source apportionment and discrimination. Sci. Total Environ. 626, 1350–1366. https://doi.org/10.1016/j.scitotenv.2018.01.192.

Sullivan, K.V., Kidder, J.A., Junqueira, T.P., Vanhaecke, F., Leybourne, M.I., 2022. Emerging applications of high-precision Cu isotopic analysis by MC-ICP-MS. Sci. Total Environ. 838, 156084 https://doi.org/10.1016/j.scitotenv.2022.156084.

Tankere-Muller, S., Zhang, H., Davison, W., Finke, N., Larsen, O., Stahl, H., Glud, R.N., 2007. Fine scale remobilisation of Fe, Mn, Co, Ni, Cu and Cd in contaminated marine sediment. Mar. Chem. 106, 192–207. https://doi.org/10.1016/j.marchem.2006.04.005.

Thapalia, A., Borrok, D.M., Van Metre, P.C., Musgrove, M., Landa, E.R., 2010. Zn and Cu isotopes as tracers of anthropogenic contamination in a sediment core from an Urban Lake. Environ. Sci. Technol. 44, 1544–1550. https://doi.org/10.1021/es902933y.

Thapalia, A., Borrok, D.M., Van Metre, P.C., Wilson, J., 2015. Zinc isotopic signatures in eight lake sediment cores from across the United States. Environ. Sci. Technol. 49, 132–140. https://doi.org/10.1021/es5036893.

Tonhá, M.S., Araújo, D.F., Araújo, R., Cunha, B.C.A., Machado, W., Portela, J.F., Pr Souza, J., Carvalho, H.K., Dantas, E.L., Roig, H.L., Seyler, P., Garnier, J., 2021. Trace metal dynamics in an industrialized Brazilian river: a combined application of Zn isotopes, geochemical partitioning, and multivariate statistics. J. Environ. Sci. 101, 313–325. https://doi.org/10.1016/j.jes.2020.08.027.

Tonhá, M.S., Garnier, J., Araújo, D.F., Cunha, B.C.A., Machado, W., Dantas, E., Araújo, R., Kutter, V.T., Bonnet, M.P., Seyler, P., 2020. Behavior of metallurgical zinc contamination in coastal environments: a survey of Zn from electroplating wastes and partitioning in sediments. Sci. Total Environ. 743, 140610 https://doi.org/10.1016/j.scitotenv.2020.140610.

Tsujimoto, A., Nomura, R., Yasuhara, M., Yoshikawa, S., 2006. Benthic foraminiferal assemblages in Osaka Bay, southwestern Japan: faunal changes over the last 50 years. Paleontol. Res. 10, 141–161. https://doi.org/10.2517/prpsj.10.141.

Wang, D., Zheng, L., Ren, M., Li, C., Dong, X., Wei, X., Zhou, W., Cui, J., 2022. Zinc in soil reflecting the intensive coal mining activities: evidence from stable zinc isotopes analysis. Ecotoxicol. Environ. Saf. 239, 113669 https://doi.org/10.1016/j.ecoenv.2022.113669.

Wang, X., Gao, N., Liang, Y., Liu, F., Hong, X., Zhou, X., Sun, L., Li, H., Fang, T., 2022. Chronological deposition record of trace metals in sediment cores from Chaohu Lake, Anhui Province, China. Environ. Monit. Assess. 194, 843. https://doi.org/10.1007/s10661-022-10506-w.

Wang, Z., Peacock, C., Kwon, K.D., Gu, X., Feng, X., Li, W., 2023. Site-specific isotope fractionation during Zn adsorption onto birnessite: insights from X-ray absorption spectroscopy, density functional theory and surface complexation modeling. Geochem. Cosmochim. Acta 348, 68–84. https://doi.org/10.1016/j.gca.2023.03.006.

Xia, Y., Liu, Y., Liu, C., Gao, T., Yin, R., Qi, M., Wu, H., 2023. Lake sediment archive reveals a distinct response to anthropogenic Pb and Zn deposition with historical periods: Pb-Zn isotope evidence. Environ. Sci. Technol. 57, 15184–15192. https://doi.org/10.1021/acs.est.3c00511.

Yan, X., Li, W., Zhu, C., Peacock, C.L., Liu, Y., Li, H., Zhang, J., Hong, M., Liu, F., Yin, H., 2023. Zinc stable isotope fractionation mechanisms during adsorption on and substitution in iron (Hydr)oxides. Environ. Sci. Technol. 57, 6636–6646. https://doi.org/10.1021/acs.est.2c08028.

Yasuhara, M., Yamazaki, H., 2005. The impact of 150 years of anthropogenic pollution on the shallow marine ostracode fauna, Osaka Bay, Japan. Mar. Micropaleontol. 55, 63–74. https://doi.org/10.1016/j.marmicro.2005.02.005.

Yokoyama, Y., Miyairi, Y., Aze, T., Yamane, M., Sawada, C., Ando, Y., de Natris, M., Hirabayashi, S., Ishiwa, T., Sato, N., Fukuyo, N., 2019. A single stage accelerator mass spectrometry at the atmosphere and ocean Research Institute, the university of Tokyo. Nucl. Instrum. Methods Phys. Res. Sect. B Beam Interact. Mater. Atoms 456, 311–316. https://doi.org/10.1016/j.nimb.2019.01.055.

Yokoyama, Y., Miyairi, Y., Matsuzaki, H., Tsunomori, F., 2007. Relation between acid dissolution time in the vacuum test tube and time required for graphitization for AMS target preparation. Nucl. Instrum. Methods Phys. Res., Sect. B 259, 330–334. https://doi.org/10.1016/j.nimb.2007.01.176.

Yoshimura, T., Takano, Y., Naraoka, H., Koga, T., Araoka, D., Ogawa, N.O., Schmitt-Kopplin, P., Hertkorn, N., Oba, Y., Dworkin, J.P., Aponte, J.C., Yoshikawa, T., Tanaka, S., Ohkouchi, N., Hashiguchi, M., McLain, H., Parker, E.T., Sakai, S., Yamaguchi, M., Suzuki, T., Yokoyama, T., Yurimoto, H., Nakamura, T., Noguchi, T., Okazaki, R., Yabuta, H., Sakamoto, K., Yada, T., Nishimura, M., Nakato, A., Miyazaki, A., Yogata, K., Abe, M., Okada, T., Usui, T., Yoshikawa, M., Saiki, T., Tanaka, S., Terui, F., Nakazawa, S., Watanabe, S., Tsuda, Y., Team, T.S.H.S., 2023. Chemical evolution of primordial salts and organic sulfur molecules in the asteroid 162173 Ryugu. Nat. Commun. 14, 5284. https://doi.org/10.1038/s41467-023-40871-0.

Zhao, M., Tarhan, L.G., Zhang, Y., Hood, A., Asael, D., Reid, R.P., Planavsky, N.J., 2021. Evaluation of shallow-water carbonates as a seawater zinc isotope archive. Earth Planet Sci. Lett. 553, 116599 https://doi.org/10.1016/j.epsl.2020.116599.

Zimmermann, T., Mohamed, A.F., Reese, A., Wieser, M.E., Kleeberg, U., Pröfrock, D., Irrgeher, J., 2020. Zinc isotopic variation of water and surface sediments from the German Elbe River. Sci. Total Environ. 707, 135219 https://doi.org/10.1016/j.scitotenv.2019.135219.